Experiments on Heat Transfer to Wires in a Partially Ionized Argon Plasma

I. KIMURA* AND A. KANZAWA†
University of Tokyo, Tokyo, Japan

The heat input rate to wires in a partially ionized atmospheric pressure argon plasma (the degree of ionization is 75% at maximum), of which temperature and stream velocity are known, was measured with an estimated accuracy of ±8%. The thermodynamic and transport properties of atmospheric pressure argon at temperatures below 20,000°K were calculated taking into consideration the effect of ionization. It was found that the incompressible empirical equations of heat and mass transfer are available for the estimation of the heat input rate in such a high temperature case. It was also shown by means of probe measurements that the boundary layers in the case of our experiments are near the frozen state and it is probable that the temperature of electrons is higher than that of atoms or ions in the boundary layers.

Nomenclature

C_v = specific heat per particle
D = wire diameter
D_{amb} = ambipolar diffusion coefficient
d = thickness of electrical sheath
E_i = energy of ionization or recombination
e = charge of electron
h = heat-transfer coefficient
h_D = mass-transfer coefficient
I = gage current
j = current density
K = thermal conductivity
K_c = as shown by Eq. (1)
K_d = as shown by Eq. (2)
K_i = mobility of ion
k = Boltzmann's constant
Le = Lewis number
$\dot{M}$ = mass-transfer rate
m = mass of particle
Nu = Nusselt number
Nu_D = Nusselt number for mass-transfer coefficient
n = number density
P_{jk} = persistence for the collision of j and k particles
Pr = Prandtl number
Q_c = convective heat input rate to wire
Q_d = diffusive heat input rate to wire
Q_e = heat loss rate of wire due to thermionic emission
Q_r = heat input rate to wire due to radiation from plasma
Q_r' = heat loss rate of wire due to radiation
Q_s = heat loss rate to supporter due to thermal conduction
Q_t = total heat input rate to wire
Q_{jk} = collision cross section for j particle → k particle
R_c = resistance of probe circuit
Re = Reynolds number
Sc = Schmidt number
T = temperature
U_{int} = internal energy of particle
$\bar{v}$ = mean velocity of particle
ΔV = potential difference in electrical sheath
λ_j = mean free path of j particle
ξ = as defined by Eq. (4)
ρ = density

Subscripts

a = atom
i = ion
e = electron
ela = elastic collision
ce = charge exchange collision

Received June 8, 1964; revision received November 30, 1964.
* Associate Professor in Aeronautics.
† Student in Postgraduate Course of Aeronautics.

I. Introduction

THE process of the heat transfer in the case of dissociated or ionized high temperature gases is complicated by the features that the thermodynamic and transport properties are greatly influenced by dissociation and ionization, and that the diffusion of atoms or ions, which subsequently recombine with a high energy release, may appreciably increase the heat-transfer rate. Some investigations on the stagnation-point heat transfer in ionized gases[1, 2] and on the heat transfer to electrodes from ionized gases[3–5] have been reported recently.

We conducted an experimental study of the heat transfer in the case where a wire is placed perpendicularly to the flow of a partially ionized atmospheric pressure argon plasma. The heat-transfer problem of such a geometry is an elementary one, and its theoretical analysis is difficult for the evaluation of the heat input rate. The purposes of the present paper are to investigate the possibility of estimating the heat input using the incompressible empirical equations of heat and mass transfer, and also to investigate the state of the gas in the boundary layers by means of probe measurements. (In this paper, we consider thermal and concentration boundary layers averaged around the wire, although a wake is formed behind it.)

II. Experimental Method and Results

Argon Arc and State of Gas in It

The experiments were performed using a direct current thermal arc in atmospheric pressure argon, arranging its electrodes vertically. The arc current is kept at 105 amp and the distance between electrodes at 5.8 mm, whereas the potential difference between them is maintained at 13.7 v.

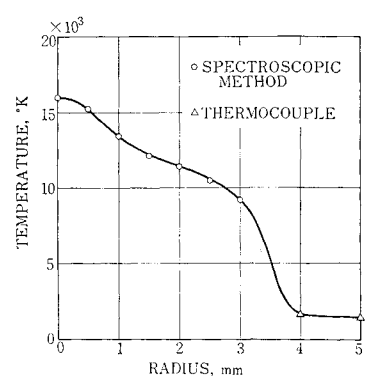

Fig. 1 Temperature distribution at a section 2 mm from the cathode in a 105-amp, 5.8-mm atmospheric pressure argon arc. Degree of ionization: at center 75% (15,900°K), 1.5-mm radius 15% (12,300°K), 3-mm radius 0.5% (9,000°K).

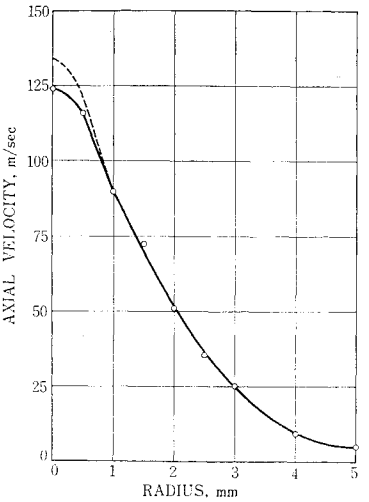

Fig. 2 Stream velocity distribution at a section 2 mm from the cathode in a 105-amp, 5.8-mm atmospheric pressure argon arc; the dotted line shows corrected result in which size of drag plate is taken into consideration.

It is shown by Olsen[6] that, except for the regions near the electrodes, the assumption of the local thermal equilibrium of the argon plasma is allowable throughout the arc column.

The measurements of the temperature and stream velocity in the arc are described in detail in Ref. 7. Figures 1 and 2, respectively, show the temperature and axial velocity distributions obtained at the section 2 mm from the tip of the cathode. In the arc, the degree of ionization extends to 75% at the center (15,900°K). The values of the viscosity given in Ref. 7 are corrected somewhat as described below, but since the effect of the correction on the data of axial velocity is very small, the data are used without any correction in the present paper. The errors in the obtained temperature and velocity are estimated to be less than 10% and 17.5%, respectively.

Measurements of Heat Input Rate

Figure 3 shows the apparatus used for the heat-transfer experiments. A tungsten (or platinum) wire supported horizontally, which is inserted into the arc by a spring, is placed at any position that is settled by spacers, in the section 2 mm from the tip of the cathode. The speed of the movement of the wire is in the order of 1 m/sec, and in the course of the movement the temperature rise of the wire is relatively small. Figure 4 shows the photograph of the arc into which a 1.0-mm-diam W wire is inserted.

The heat input rate to wires is measured by recording their resistance variations with time, using an electromagnetic oscilloscope. The resistance measuring circuit is floated electrically from the power source of the arc, so it is free from the electrical disturbance when the wire comes in contact with the

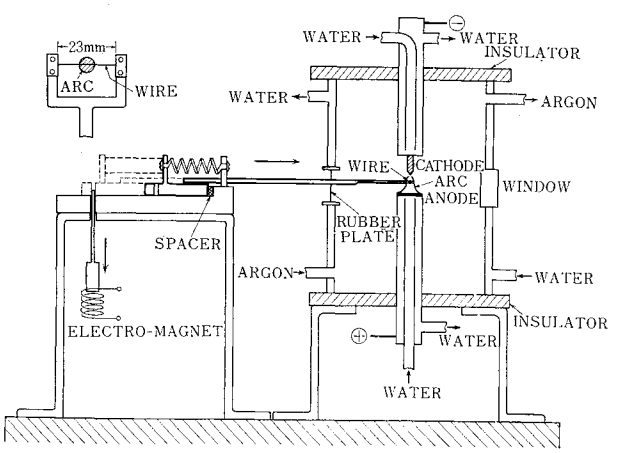

Fig. 3 Apparatus of heat-transfer experiments.

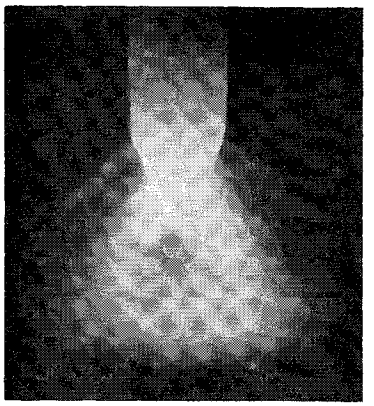

Fig. 4 Photograph of a 105-amp, 5.8-mm atmospheric pressure argon arc, into which a 1.0-mm-diam W wire is inserted.

arc. Figure 5 shows the oscillogram in the case where a 0.5-mm-diam W wire was placed in the arc. It is seen in the oscillogram that the heat input rate is almost constant for some time after the stoppage of the wire (its time is shown by the arrow). Such a tendency, that is observed in all oscillograms obtained, may be explained by the fact that the temperature difference between the arc plasma and wires is very large compared with the temperature change in wires. When the wire is inserted, a little variation of potential difference between cathode and anode is observed in the oscillogram, but the variation of arc current was hardly noticed, since the value of the current is settled mainly by the stabilizing resistance. It is also confirmed by motion picture records that the aspect of the arc discharge does not undergo a noticeable change by inserting the wire.

The variations of the heat input rate (Q_t) with the position of wires are shown in Fig. 6 for three wire diameters (D). In this figure, the curves are arranged so that their maxima coincide with the origin of the abscissa. The error in the heat input rate obtained is estimated to be less than 8%, taking into account some ambiguity of the specific resistance of tungsten at high temperatures. It is reported that when the heat input rate to wires, which is extremely high, is measured by the present method, the result of its measurement varies with gage current $(I)^4$, but as shown in the figure, such a fact is not observed in the range of the heat input rate of our experiments.

A second experimental method is then applied to insure the reliability of the results of the forementioned measurements. A 0.5-mm-diam W wire supported horizontally is swept across the arc in the forementioned section, and using the same method as already described, the heat input rate is obtained at any time. Figure 7 shows the value of the heat input rate obtained when the moving wire is just at the center of the arc, taking the sweep velocity to the abscissa. In the figure, the value for the zero sweep velocity is taken from the data shown in Fig. 6. It is seen that the obtained value of the heat input rate is kept constant for the sweep velocity, and this fact suggests that the inevitable oscillation of wires due to the sudden stoppage in the first experiments and the

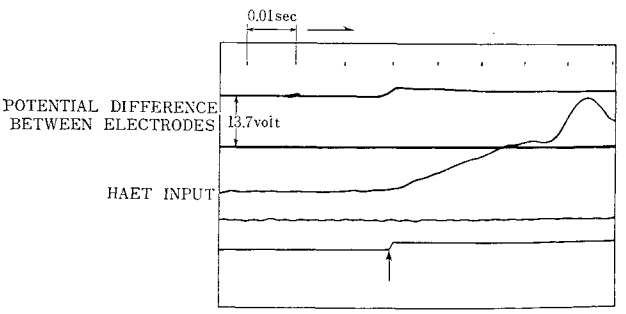

Fig. 5 Oscillogram of resistance variation (heat input) of a 0.5-mm-diam W wire placed in the arc.

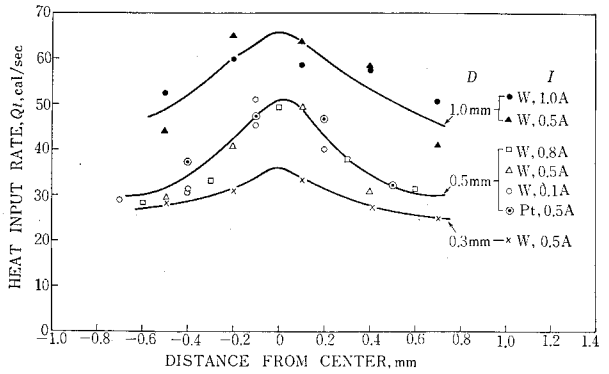

Fig. 6 Variations of heat input rate to wires with their position in the section 2 mm from the cathode of the arc of which degree of ionization is 75% at maximum; *D*: wire diameter, I: gage current.

aerodynamical disturbance caused in the arc by moving wires do not cause any noticeable effect on the measurements.

Probe Measurements

In order to study the state of the gas in the boundary layers formed around wires, the probe measurements as proposed by Langmuir were made. A wire probe, a 0.5-mm-diam *W* wire, is swept across the arc in the forementioned section with the speed of about 30 cm/sec, and currents to the wire for various wire potentials are measured, using the circuit shown in Fig. 8. Figure 9 shows the potential-current relations obtained when the moving wire is just at the center of the arc. It seems that sudden changes exist in the potential-current characteristics, such as noticed by Fragstein,[8] in the vicinity of 9 v. (Fragstein's experiment is that conducted using atmospheric pressure arc.) It is confirmed, for low-density plasmas, that such a change occurs at the plasma potential, and it is considered that it is caused by the transition of the electrical sheath from ions to electrons. We suppose that since these circumstances are the same for high density plasmas, it will be allowable to assume that the plasma potential in the present experiment is approximately 9 v from the cathode. It was noticed that the potential-current characteristics change to some extent with the wire temperature that depends on the sweep speed, but on this phenomenon no detailed study was made, since the knowledge on it is not required necessarily in the discussions described below.

III. Thermodynamic and Transport Properties

In this section, we will give the thermodynamic and transport properties of high-temperature argon of atmospheric pressure, which are used in the next section. In the present calculation doubly charged ions or more are ignored, since under 20,000°K the number density of them is usually very small. The thermodynamic and transport properties of a partially ionized monoatomic gas under a constant pressure

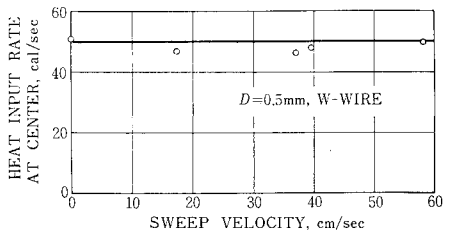

Fig. 7 Heat input rate to a 0.5-mm-diam wire for sweep velocity when the moving wire is just at the center of the arc.

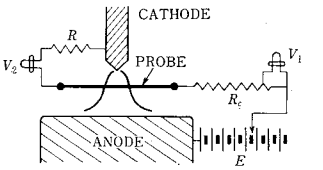

Fig. 8 Circuit used for probe measurements.

are functions of the composition and the temperatures of species involved (atoms, ions, and electrons) generally, although these properties in the equilibrium case are decided by the temperature only.

Composition and Density

The composition and density of atmospheric pressure argon in the thermal equilibrium are calculated by using the Saha equation in combination with the perfect gas equation.

Specific Heat

The equilibrium specific heat of the gas is calculated by the conventional method, taking into consideration the energies of translation, excitation, and ionization. Figure 10 shows the calculated result of the equilibrium specific heat at atmospheric pressure. The frozen specific heat is calculated, taking into consideration the energies of translation and excitation. The necessary spectroscopic data in these calculations are taken from Ref. 9.

Thermal Conductivity

The equilibrium thermal conductivity of the gas is obtained from the sum of K_c and K_d, which is expressed as follows[10, 11]:

$$K_c = \sum_j \frac{1}{3} n_j \lambda_j C_{vj} \bar{v}_j \tag{1}$$

$$K_d = \rho D_{\text{amb}} (1/m_a)(d\xi/dT)\{\tfrac{5}{2} kT + E_i + (U_{\text{int},i} - U_{\text{int,a}})\} \tag{2}$$

where

$$\frac{1}{\lambda_j} = \sum_k \left(1 - \frac{1}{2} P_{jk}\right) n_k Q_{jk} \left\{1 + \left(\frac{m_j}{m_k}\right)\right\}^{1/2} \tag{3}$$

$$\xi = (1/\rho)(n_e m_e + n_i m_i) \tag{4}$$

D_{amb} in Eq. (2) is the ambipolar diffusion coefficient expressed by Eq. (5) shown later. The values of necessary collision cross sections are obtained as described below. Q_{aa} is evaluated from the property values given by Amdur and Mason,[12] and $Q_{ia,\text{ela}}$ or $Q_{ai,\text{ela}}$ (elastic collision cross section between

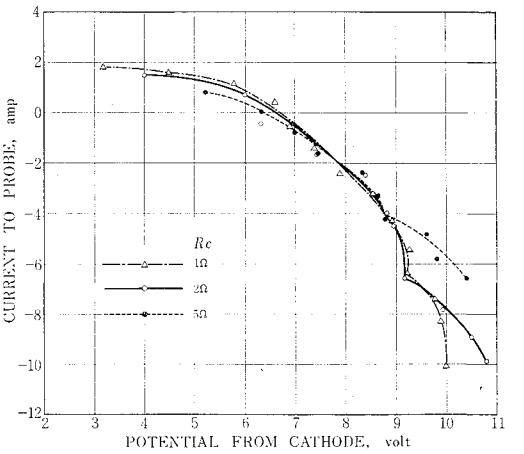

Fig. 9 Results of probe measurements.

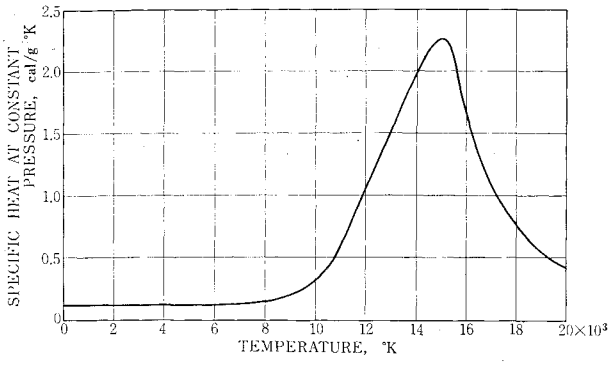

Fig. 10 Variation of equilibrium specific heat of atmospheric pressure argon with temperature.

atom and ion) is assumed to be equal to Q_{aa}. $Q_{ia,ce}$ or $Q_{ai,ce}$ (charge exchange cross section) is taken from Ref. 1, and, for Q_{ea}, Ramsauer cross section of 2×10^{-16} cm^2 is used, and Q_{ii}, Q_{ei}, or Q_{ee} is calculated by the slightly modified Gvosdover formula[13] expressed by $(e^4/k^2T^2)\ \ln(kT/e^2n^{1/3})$. The collision of ion → electron and atom → electron can be neglected in the calculations of the effective mean free paths of ions and atoms, since the factor of the persistence in Eq. (3) can be regarded as zero because m_i or $m_a \gg m_e$. The quoted charge exchange cross section was used only for the calculation of D_{amb}. Figure 11 shows the calculated result of the equilibrium thermal conductivity. The values of the frozen thermal conductivity are calculated by Eqs. (1) and (3), deciding the values of the cross sections in the same manner.

Viscosity

The method of the calculation of the equilibrium and frozen viscosities is substantially the same as that in Ref. 7, except that Q_{aa} is evaluated from the property values given by Amdur and Mason. Figure 12 shows the calculated result of the equilibrium viscosity.

Ambipolar Diffusion Coefficient

The ambipolar diffusion coefficient D_{amb} is calculated by

$$D_{\text{amb}} = \frac{2}{3}\left(\frac{n_a\lambda_i\bar{v}_i + n_i\lambda_a\bar{v}_a}{n_a + n_i}\right) \tag{5}$$

where λ_i and λ_a are calculated from Eq. (3), excluding self-collision cross sections.[10] In the case where the temperature of electrons is higher than that of ions, the following equation is used for the evaluation of D_{amb}[14]:

$$D_{\text{amb}} = \frac{1}{3}\left(1 + \frac{T_e}{T_i}\right)\left(\frac{n_a\lambda_i\bar{v}_i + n_i\lambda_a\bar{v}_a}{n_a + n_i}\right) \tag{5a}$$

IV. Discussions

Evaluation of Heat Input Rate by Incompressible Empirical Equations

The total heat input rate (Q_t) to a floating wire placed in a flowing plasma will be expressed by

$$Q_t = Q_c + Q_d + Q_r - Q_r' - Q_e - Q_s \tag{6}$$

where Q_c is convective heat input rate, Q_d is diffusive heat input rate (due to the recombination of ions and electrons that arrive at the wall by ambipolar diffusion), Q_r is heat input rate due to the radiation from the plasma, Q_r' is heat loss rate due to the radiation of the wire, Q_e is heat loss rate due to thermionic emission, and Q_s is heat loss rate to the supporter of the wire due to the thermal conduction. The electrical sheath (its thickness is discussed later), which is

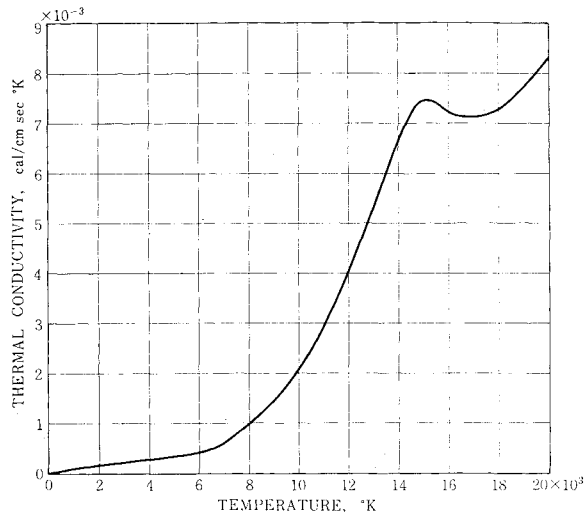

Fig. 11 Variation of equilibrium thermal conductivity of atmospheric pressure argon with temperature.

formed at the bottom of the boundary layers, is not taken into consideration in the evaluation of heat input rate, since in the case of a floating wire the potential difference across it is not large and its effect on the heat transfer is small. It can be shown in the present case that in Eq. (6), Q_r, Q_r', Q_e, and Q_s are negligibly small (for a 0.5-mm-diam W wire the estimated upper-limit values of Q_r, Q_r', Q_e, and Q_s are 1.2 cal/sec, 0.5 cal/sec, 0.01 cal/sec, and 0.4 cal/sec, respectively), so the next relation holds approximately:

$$Q_t = Q_c + Q_d \tag{6a}$$

A trial of the evaluation of Q_t by calculations will be made in the case where the wires are placed at the center in the forementioned section of the arc, using the conventional incompressible empirical equations. Since the temperature and velocity in the arc vary with radial distance, the calculations are conducted separately on the individual parts of 0.5-mm length of the wire, assuming a wire temperature distribution that is 1000°K constant over 7 mm in the middle part of the wire and ambient temperature in the other part. (The calculated values of Q_t were hardly affected by the form of the wire temperature distribution.) For the calculation of ambipolar mass-transfer rate, it is assumed that the wall of the wire is fully catalytic and that the concentration of ions or electrons of the gas at the outer edge of the concentration boundary layer is equal to that of the gas in the thermal equilibrium at the temperature of the outer edge of the corresponding thermal boundary layer.

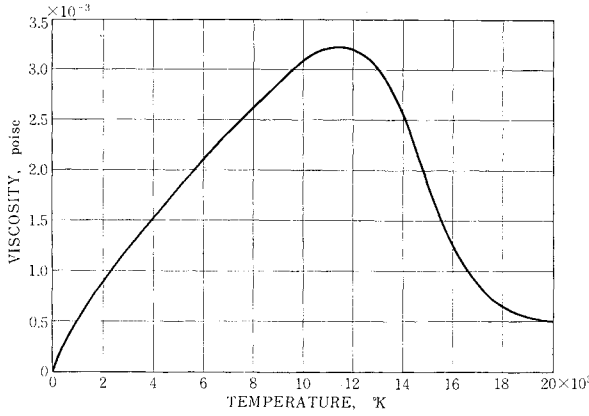

Fig. 12 Variation of equilibrium viscosity of atmospheric pressure argon with temperature.

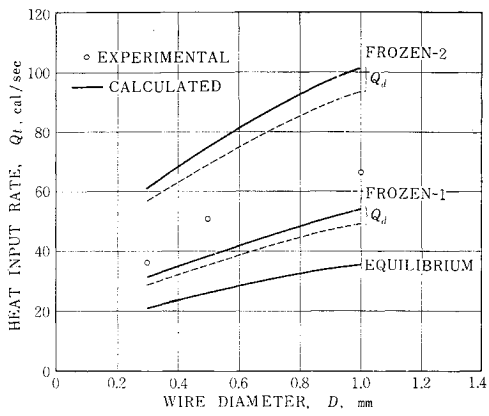

Fig. 13 Variations of heat input rate with wire diameter, when wires were placed at the center in the section 2 mm from the cathode of the arc of which degree of ionization is 75% at maximum; full line: Q_t, dotted line: Q_c.

Under the assumption of frozen boundary layers (very slow recombination rates), the convective and diffusive heat input rates can be calculated independently. The convective heat input rate (Q_c) is estimated by the empirical heat-transfer equation[15]

$$Nu = hD/K = (0.35 + 0.47Re^{0.52})Pr^{0.3} \tag{7}$$

inserting the frozen property values at a reference temperature corresponding to the arithmetic mean of the gas temperature at the outer edge of the thermal boundary layer and the wall temperature, and at a reference composition corresponding to the gas at the position where the temperature is equal to the forementioned reference temperature. The ambipolar mass-transfer rate ($\dot{M}$) is estimated by the empirical mass-transfer equation

$$Nu_D = h_D D/D_{amb} = (0.35 + 0.47Re^{0.52})Sc^{0.3} \tag{8}$$

inserting the frozen property values at a reference composition with the concentration of ions or electrons corresponding to the arithmetic mean of the concentration at the outer edge of the concentration boundary layer and that at the wall (zero for a fully catalytic wall), and at a reference temperature corresponding to the gas at the position where the composition is equal to the forementioned reference composition. Then, the diffusive heat input rate (Q_d) is obtained by

$$Q_d = E_i\dot{M} \tag{9}$$

where E_i is the energy of recombination.

To obtain the reference composition in the calculation of Q_c or the reference temperature in the calculation of Q_d, the ratio of concentration and temperature boundary-layer thicknesses was estimated at $Le^{1/3}$ evaluated at the reference temperature and composition corresponding to the arithmetic mean, and the distributions of temperature and concentration in the boundary layers were assumed in the form of the conventional cubic expression. It must be noticed that the value of Lewis number in this case is much smaller than 1, since the increase of electrons in the gas increases the thermal conductivity of it remarkably. The order of Reynolds number related to a 0.5-mm wire diameter is 50 for the stream at the central part of the arc.

In Fig. 13, the sum of Q_c and Q_d calculated in the foregoing manner is shown as "Frozen-1," taking wire diameter to the abscissa. In the figure, "Frozen-2" is of the case where it is assumed in the evaluation of properties that over the boundary layers the electron temperature is equal to the gas temperature at the outer edge of the thermal boundary layer. It is seen in the figure that the value of Q_c is considerably larger than that of Q_d generally.

Under the assumption of equilibrium boundary layers (fast recombination rates), Q_c is estimated using Eq. (7), inserting the equilibrium property values at a reference temperature corresponding to the arithmetic mean. In this case, it can be shown that Q_d is negligibly small compared with Q_c. In Fig. 13, Q_t ($\cong Q_c$) calculated in this manner is shown as "equilibrium."

In the figure, the experimental values taken from Fig. 6 are also plotted. The calculated results seem to be satisfactory in agreement with the experimental results, taking into consideration that the real boundary layers are near the frozen state and the temperature of electrons in the boundary layers is higher than that of atoms or ions there as described in the following section. (The error in the calculated results caused by errors in the temperature and stream velocity data is less than 20%.)

State of Gas in Boundary Layers

In this experiment, the thickness of the electrical sheath, which is of the order of the Debye distance, is far smaller than the thicknesses of the boundary layers. The results of probe measurements shown in Fig. 9 can be used to investigate the state of the gas at the bottom of the boundary layers, and the result of such an investigation suggests that the boundary layers in the present experiment are near the frozen state, as described below.

It is known that in the case where the collisionless model as proposed by Langmuir is valid, the following equations hold for a negative probe:

$$j_i = \frac{1}{4} n_i \bar{v}_i e = \frac{1}{9\pi}\left(\frac{2e}{m_i}\right)^{1/2} \frac{\Delta V^{3/2}}{d^2} \tag{10}$$

$$j_e = \frac{1}{4} n_e \bar{v}_e e \exp[-e\Delta V/kT_e] \tag{11}$$

For the problems in the case where the density and degree of ionization are such that the collision in the electrical sheath is not negligible, several investigations based on the continuum theory have been reported recently.[16, 17] In the present problem, it must be noticed that for the cases of the frozen and equilibrium boundary layers, the Debye distances related to the state of the gas at the bottom of them differ considerably from each other, since the number densities of charged particles are very different in both cases.

At first, under the assumption of equilibrium boundary layers, the theoretical estimation of ion current collected by a 0.5-mm-diam wire placed at the center in the forementioned section of the arc will be made. As the densities of charged particles in the bottom of the boundary layers are very low in the equilibrium case, the thickness of the electrical sheath (Debye distance) is generally so large that the collisionless model is not applicable. Therefore, the following equation, which was derived in the same manner as Eq. (10) considering collisions in the electrical sheath, is used here[18]:

$$j_i = \frac{1}{4} n_i \bar{v}_i e = \frac{9K_i}{32\pi} \frac{\Delta V^2}{d^3} \tag{10a}$$

Assuming the same wire temperature distribution as that in the case of the evaluation of the heat input rate, the temperature field in the vicinity of the wall of any individual part of 0.5-mm length of the wire can be decided, since the heat input rate to the part is already obtained. Then, using Eq. (10a), the value of ion current to the part is obtained for a given wire potential. When the wire potential is 6 v below the plasma potential, the calculated total ion current takes the value of 0.015 amp, which is far smaller than that expected from the results of the probe measurements (the experimental results shown in Fig. 9 suggest that the ion current collected by the wire is in the order of 1 amp when its potential is slightly negative). On the other hand, under the assumption of frozen boundary layers, it is shown that the

ions arrive at the wall by the ambipolar diffusion at a rate corresponding to about 1.3 amp, when the wire is at the plasma potential, and this matter, which is considered to be valid for the slightly negative potential, as well as the plasma potential, is compatible with the suggestion of the results of the probe measurements. Thus, it will be reasonable to assume that the boundary layers in the present experiment are near the frozen state.

Since the boundary layers in the present experiment are near the frozen state, the densities of charged particles in the bottom of the boundary layers are fairly high and the corresponding Debye distance becomes small. Under the assumption of $T_e = T_i$, the thickness of the electrical sheath estimated using Eq. (31) of Ref. 17, which was derived on the basis of continuum theory, takes the value of 5×10^{-5} cm, whereas the order of the mean free path of ions or electrons in the bottom of the boundary layers is 10^{-5} cm. (In this case the collision cross section between charged particles given by the Gvosdover formula becomes very large, since the temperature is low.) On the other hand, considering that in the boundary layers the temperature of electrons does not decrease in accordance with that of ions or atoms, the mean free path of electrons in the bottom of the boundary layers becomes comparable to the thickness of the electrical sheath or more. (For the electrons of 10⁴°K, the mean free path in the bottom of the boundary layers is in the order of 10^{-3} cm.) On the basis of such a consideration, we tried to estimate the electron temperature at the outer edge of the electrical sheath from the data shown in Fig. 9, using Eq. (11). (In this case it is assumed that, for the change of the electron current density, the effect of the factor $\exp[-e\Delta V/kT_e]$ in the right side of the equation is dominant.) The result of such an investigation showed that the mean electron temperature is about 10,000°K there. Although the accuracy of it is not satisfactory, this fact seems to suggest that the temperature of electrons in the boundary layers is higher than that of atoms or ions there.

References

[1] Fay, J. A. and Kemp, N. H., "Theory of stagnation-point heat-transfer in a partially ionized diatomic gas," AIAA J. **1,** 2741–2751 (1963).

[2] Rose, P. H. and Stankevics, J. O., "Stagnation-point heat-transfer measurements in partially ionized air," AIAA J. **1,** 2752–2763 (1963).

[3] Schoeck, P. A. and Eckert, E. R. G., "Experiments on the transpiration cooled anode of an electric arc," *Proceedings of the Heat Transfer and Fluid Mechanics Institute* (Stanford University Press, Stanford, Calif., 1961), pp. 193–207.

[4] Fay, J. A. and Hogan, W. T., "Heat transfer to cold electrodes in a flowing ionized gas," Phys. Fluids **5,** 885–890 (1962).

[5] Schoeck, P. A., "An investigation of the anode energy balance of high intensity arcs in argon," *Modern Developments in Heat Transfer* (Academic Press, New York, 1963), pp. 353–400.

[6] Olsen, H. N., "Thermal and electrical properties of an argon plasma," Phys. Fluids **2,** 614–623 (1959).

[7] Kimura, I. and Kanazawa, A., "Measurement of stream velocity in an arc," AIAA J. **1,** 310–314 (1963).

[8] Fragstein, C. v. and Arndt, M., "Untersuchungen über die Sondenmessmethode in Kohlebogen bei Atmosphärendruck," Ann. Phys. **33,** 532–564 (1938).

[9] Moore, C. E., "Atomic energy levels I," National Bureau of Standards Circular 467 (1949), pp. 211–216.

[10] Edels, H. and Craggs, J. D., "The coefficients of thermal and electrical conductivity in high temperature gases," Progr. Dielectrics **5,** 188–231 (1963).

[11] Burhorn, F., "Berechnung und Messung der Wärmeleitfähigkeit von Stickstoff bis 13,000°K," Z. Physik **155,** 42–58 (1959).

[12] Amdur, I. and Mason, E. A., "Properties of gases at very high temperatures," Phys. Fluids **1,** 370–383 (1958).

[13] Maecker, H., Peters, Th., and Schenk, H., "Ionen- und Atomquerschnitte im Plasma verschiedener Gase," Z. Physik **140,** 119–138 (1955).

[14] Simon, A., *An Introduction of Thermonuclear Research* (Pergamon Press, Oxford, England, 1959), pp. 154–160.

[15] McAdams, W. H., *Heat Transmission* (McGraw-Hill Book Co., Inc., New York, 1954), pp. 258–261.

[16] Su, C. H. and Lam, S. H., "Continuum theory of spherical electrostatic probes," Phys. Fluids **6,** 1479–1491 (1963).

[17] Turcotte, D. L. and Gillespie, J., "Electrical resistance and sheath potential associated with a cold electrode," AIAA J. **1,** 2293–2299 (1963).

[18] Engel, A. v., *Ionized Gases* (Clarendon Press, Oxford, England, 1955), pp. 11–21.